Electrochemiluminescence Enhancement and Particle Structure Stabilization of Polymer Nanoparticle by Doping Anionic Polyelectrolyte and Cationic Polymer Containing Tertiary Amine Groups and Its Highly Sensitive Immunoanalysis

Authors:

Noor Ul Ain, Tian-Yu Wang, Xiao-Ning Wu, Tong-Hong Wei, Jing-Shuo Zhang, Hong-Ping Xie

Date Submitted: 2021-02-22

Keywords: immunoanalysis, doping, ionic polymer, particle structure stabilization, signal enhancement, electrochemiluminescence nanoparticle

Abstract:

A doped polymer nanoparticle (dPNP) of electrochemiluminescence (ECL) was prepared via doping the anionic polyelectrolyte polyacrylic acid (PAA) and the cationic polymer poly-ethyleneimine (PEI) into the polymer nanoparticle (PNP), which was self-assembled by Ru(bpy)32+ derivative-grafted PAA (PAA?Ru) with both cations and anions. The good electrical conductivity of the doped polyelectrolyte PAA enhanced the ECL intensity of PNP to 109.1%, and the involvement of a large number of tertiary amine groups of the doped PEI further enhanced that to 127.3%; meanwhile, doping low-molecular-weight PEI into PNP, while simultaneously doping high-molecular-weight PAA, avoided the precipitation of PAA and PEI, due to interaction of the two oppositely charged polymers; and these also made the self-assembly procedure more effective and the nanoparticle structure more stable than PNP and also led to the production of rich residual PAA chains on the surface of dPNP. The storage results showed that the average hydrated particle diameter kept almost constant (197.5?213.1 nm) during 15-day storage and that the nanoparticles have rich surface charge of ?11.47 mV (zeta potential), well suspension stability and good dispersity without detectable aggregation in the solution during the storage. Therefore, the nanoparticle is quite suitable for the antibody labeling, immunoassay and the storage. As a result, a high-sensitive ECL immunoassay approach with good precision, accuracy and selectivity was established and an ultra-low detection limit of 0.049 pg mL?1 (S/N = 3) for magnetic bead-based detection of Hepatitis B surface antigen was observed.

Record Type: Published Article

Submitted To: LAPSE (Living Archive for Process Systems Engineering)

Citation (overall record, always the latest version):	LAPSE:2021.0045
Citation (this specific file, latest version):	LAPSE:2021.0045-1
Citation (this specific file, this version):	LAPSE:2021.0045-1v1

DOI of Published Version: https://doi.org/10.3390/pr8091054

processes

MDPI

Article

Electrochemiluminescence Enhancement and Particle Structure Stabilization of Polymer Nanoparticle by Doping Anionic Polyelectrolyte and Cationic Polymer Containing Tertiary Amine Groups and Its Highly Sensitive Immunoanalysis

Noor Ul Ain †, Tian-Yu Wang †, Xiao-Ning Wu, Tong-Hong Wei, Jing-Shuo Zhang * and Hong-Ping Xie *

College of Pharmaceutical Sciences, Soochow University, Suzhou 215123, China; noorulain22@yahoo.com (N.U.A.); 20195226022@stu.suda.edu.cn (T.-Y.W.); xiaoning_wu123@163.com (X.-N.W.); piers.wei@abbott.com (T.-H.W.)

* Correspondence: zhangjingshuo@suda.edu.cn (J.-S.Z.); hpxie@suda.edu.cn (H.-P.X.)

† Who had the equal contribution to this paper.

Received: 27 July 2020; Accepted: 21 August 2020; Published: 28 August 2020

Abstract: A doped polymer nanoparticle (dPNP) of electrochemiluminescence (ECL) was prepared via doping the anionic polyelectrolyte polyacrylic acid (PAA) and the cationic polymer poly-ethyleneimine (PEI) into the polymer nanoparticle (PNP), which was self-assembled by $Ru(bpy)_3^{2+}$ derivative-grafted PAA (PAA–Ru) with both cations and anions. The good electrical conductivity of the doped polyelectrolyte PAA enhanced the ECL intensity of PNP to 109.1%, and the involvement of a large number of tertiary amine groups of the doped PEI further enhanced that to 127.3%; meanwhile, doping low-molecular-weight PEI into PNP, while simultaneously doping high-molecular-weight PAA, avoided the precipitation of PAA and PEI, due to interaction of the two oppositely charged polymers; and these also made the self-assembly procedure more effective and the nanoparticle structure more stable than PNP and also led to the production of rich residual PAA chains on the surface of dPNP. The storage results showed that the average hydrated particle diameter kept almost constant (197.5–213.1 nm) during 15-day storage and that the nanoparticles have rich surface charge of −11.47 mV (zeta potential), well suspension stability and good dispersity without detectable aggregation in the solution during the storage. Therefore, the nanoparticle is quite suitable for the antibody labeling, immunoassay and the storage. As a result, a high-sensitive ECL immunoassay approach with good precision, accuracy and selectivity was established and an ultra-low detection limit of 0.049 pg mL^{-1} (S/N = 3) for magnetic bead-based detection of Hepatitis B surface antigen was observed.

Keywords: electrochemiluminescence nanoparticle; signal enhancement; particle structure stabilization; ionic polymer; doping; immunoanalysis

1. Introduction

Immunoanalysis has been widely used in clinical, medical and pharmaceutical investigation [1–5]. In clinical assay, electrochemiluminescence (ECL) immunoanalysis using ruthenium complex $Ru(bpy)_3^{2+}$, as luminophore, is most widely used owing to its higher sensitivity and wider linear range [6–8]. However, increasing labeling amount of ECL tag and enhancing signal are two keys for ECL immunoanalysis.

Due to lack of active groups, the naked $Ru(bpy)_3^{2+}$ is unable to be used as a bio-labelling tag. As a solution, the derivatives of $Ru(bpy)_3^{2+}$ and the $Ru(bpy)_3^{2+}$ immobilized nanoparticles are usually used as signal tag [8–21]. The derivatives of $Ru(bpy)_3^{2+}$ can directly label detector antibody, but their labelling amount on the detector antibody is limited, and then the signal amplification ability is also limited. Nanoparticle, especially silica one, can provide significant signal amplification, due to easy surface modification, porous structure and large surface area [10–22]. There are two main approaches for immobilization of ruthenium complex, i.e., the internal immobilization based on micropore adsorbing or doping [10–17] and the surface immobilization via cation-exchanging or covalent conjugating [13,17–22]. Usually, poor electric conductivity of the nanoparticles reduces the electron transfer ability between the working electrode and the ECL active molecules immobilized inside the nanoparticle. Though the surface immobilization could overcome the poor electrical conductivity, the surface-based load capacity is usually lower than the former. Our study group proposed an ECL enhanced approach by doping the ion-pair macromolecules PAA–$Ru(bpy)_3^{2+}$ [17], where PAA is anionic polyelectrolyte polyacrylic acid. Due to a large number of negative charges on the long chain of PAA molecule, one PAA molecule can adsorb a large number of the cationic small molecules $Ru(bpy)_3^{2+}$ to form one ECL ion-pair macromolecule. Hence, the approach significantly increased the loading capacity of $Ru(bpy)_3^{2+}$, as well as enhanced the internal electron transfer ability owing to good electrical conductivity of doped polyelectrolyte. A sensitive ECL immunoanalysis approach has been established based on the signal-enhanced nanoparticle [17]. However, electrostatic interaction-based immobilization for $Ru(bpy)_3^{2+}$ is not beneficial to the ECL stability.

Immobilization of the capturer antibody has also a significant inference on the sensitivity of ECL based immunoassay. Nanomaterial doped sensing membrane based ECL sensor has been widely focused [19,23–33], including carbon nanotubes [19,23–25], graphene [30,31] and gold nanoparticles [19,26–30,32,33]. Because the sensing membrane and capturer antibodies all are directly immobilized on the surface of working electrode, this kind of sensor has both a good electrical conductivity and a large immobilizing amount of the capturer antibody. Hence, there is a high detecting sensitivity, and their detecting limits may be as low as pg (picogram) or fg (femtogram) per milliliter. However, this kind of sensors is difficult to match the requirement of an automated detection of the large number of samples in clinical assay. In fact, clinical assay usually uses magnetic bead (MB) to immobilize capturer antibody, and the corresponding detected immune complex containing MB is attracted to the surface of the working electrode by a strong magnet. Here the electrode is only used as an exciting tool of ECL. It is noticeable that the strength of the interaction between the immune assay complex and the working electrode is weak and that the load capacity of the capturer antibody is also low, compared to the above sensing membrane [19–32]. Hence, the magnetic bead-based detecting sensitivity is usually much lower than the sensing membrane based one. However, the MB-based automatization is more necessary in clinical detection assay.

Based on the above reviews, a highly sensitive MB-based ECL immunoanalysis method with potential for clinical application should have a suitable ECL nanoparticle as signal tag, with enhanced ECL intensity, as well as a stable particle structure. To realize the objective, based on our previous research results about the good electrical conductivity of polyelectrolyte PAA doped in ECL nanoparticle, a collective self-assembly approach was proposed, including $Ru(bpy)_3^{2+}$ derivative grafted PAA (PAA–Ru), PAA and cationic polymer poly-ethyleneimine (PEI) with a very low molecular weight and rich positive charges and the basic principle is shown in Figure 1. Due to the good electrical conductivity of PAA and a large number of tertiary amine groups of PEI, PAA and PEI doped PAA–Ru self-assembled polymer nanoparticle, called as dPNP, will have a significantly enhanced ECL. At the same time, the long molecular chain of PAA with rich negative charges and the short molecular chain of PEI with rich positive charges will significantly enhance electrostatic interaction of the long molecular chains of the self-assembled PAA–Ru with both negative charges and positive ones each other and then will significantly increase the structure stability of the ECL nanoparticle. Compared with the short molecular chain of PEI, the long chain of PAA will lead to that the PAA residual chains appear

on the surface of the nanoparticle, where they provide carboxyl group for antibody labeling and a spacer between the labeled antibody and the body core of the nanoparticle. Hence, the as-prepared nanoparticle is suitable for the antibody labeling and the immunoassay, and the MB-based high sensitivity ECL immune-analysis approach is established in this study.

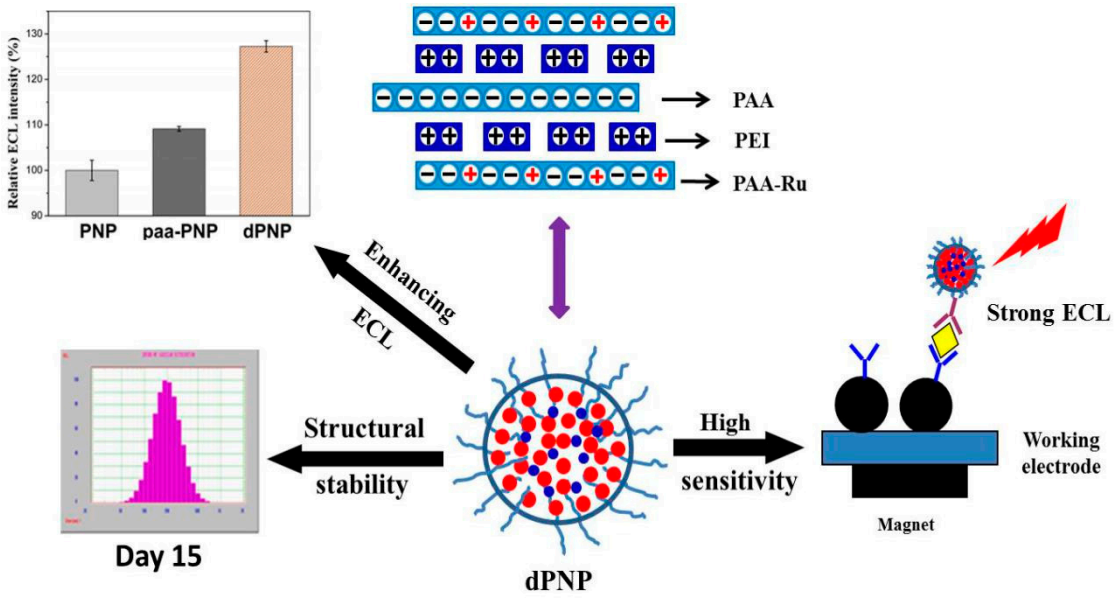

Figure 1. Schematic diagram of preparation of a doped polymer nanoparticle (dPNP), its electrochemiluminescence (ECL) enhancement and structural stability and principle of dPNP-based sensitive immune-assay. Here polymer nanoparticle (PNP) was the $Ru(bpy)_3^{2+}$ derivative-grafted polyacrylic acid (PAA–Ru) self-assembled nanoparticle, and paa-PNP was polyacrylic acid PAA doped PNP.

2. Materials and Methods

2.1. Materials and Instruments

Branched poly ethyleneimine (Mw = 1800, 99% *w/w*) and polyacrylic acid (Mw = 100,000, 35%, *w/w*) were purchased from Sigma-Aldrich. Tripropylamine (TPA) (≥98%, *w/w*) was purchased from Sinopharm Chemical Reagent Co., Ltd. Magnetic bead-conjugated goat anti-mouse IgG (mIgG–MB), magnetic bead-conjugated goat anti-rabbit IgG (rIgG–MB), bovine serum albumin (BSA) and dialysis bag (MWCO 3.5KD) were purchased from the Sangon Biotech (Shanghai, China) Co., Ltd. Goat anti-HBsAg monoclonal antibody (gAb), mouse anti-HBsAg antibody (mAb) and HBsAg were purchased from Zhengzhou Yikang Biologic Engineering Co., Ltd. (Zhengzhou, China). Rabbit anti-goat IgG (gIgG) was purchased from BOSTER Biologic Technology Co., Ltd. (Wuhan, China). Other chemicals were in analytical grade or higher grades. The water used during experiment was triple-distilled deionized water made by our laboratory.

UV-vis spectrophotometer (UV-2401PC, SHIMADZU Company, Kyoto, Japan), fluorescence spectrophotometer (LS-55, PerkinElmer Company, Waltham, MA, USA), Transmission electron microscope (TEM, H-600, Hitachi, Japan,), Laser particle size analyzer (Nicomp380 AccuSizer780, PSS, Port Richey, FL, USA), Electrochemiluminescence analyzer (MPI-A, Xi'an Remax Electronic Science & Technology Co., Ltd., Xi'an, China).

2.2. Synthesis of ECL Polymer and Preparation of Doped Polymer Nanoparticle

First, the ECL complex bis (2,2-bipyridine)–(5,6-epoxy-5,6-dihydro-[1,10] phenanthroline) ruthenium (epo–Ru, see Figure S1 of supporting information) grafted PAA (PAA–Ru) was synthesized

(Seen in Section S2 of Supporting Information). After that, the PAA and PEI doped polymer nanoparticle dPNP would be prepared by using the synthesized PAA–Ru. Briefly, in a round-bottom flask containing 2.1 mL deionized water, 0.3-mL PAA solution (0.174 mg mL^{-1}) was added under ultrasound condition. Then, 0.3-mL PEI solution (0.0208 mg mL^{-1}) and 0.3-mL PAA–Ru DMF solution was quickly dripped separately. After 15 min of continuous ultrasound treatment, the dPNP solution was obtained and stored at room temperature for next use. ECL detection of dPNP was carried out according to Section S3 of Supporting Information.

2.3. Labeling Detector Antibody and Immobilizing Capturer Antibody

Labeling of detector antibody: First, the surface carboxyl of dPNP was activated according to the approach in Section S4 of Supporting Information. Then, 200 μL of carboxyl activated dPNP solution was taken into an EP tube blocked by BSA, then 100 μL of second antibody rabbit anti-goat IgG (gIgG, 50 μg mL^{-1}) was added and incubated at 37 °C for 2 h. After that, 100 μL of 1% BSA was added and incubated at 37 °C for 60 min to block nonspecific binding site of dPNP, the ECL nanoparticle-labeled secondary antibody (dPNP–gIgG) was prepared. Next, 100 μL of first antibody goat anti-HBsAg monoclonal antibody (gAb, 50 μg mL^{-1}) was then added. After incubating at 37 °C for 30 min, the immune complex dPNP–gIgG–gAb, abbreviated as dPNP–gAb, was formed, and then the ECL nanoparticle-labeled detecting probe, called as the detecting probe, was prepared.

Immobilizing capturer antibody on magnetic bead: 20 μL of second antibody IgG immobilized magnetic beads mIgG–MB (a commercial magnetic bead-conjugated goat anti-mouse IgG, 0.4 mg protein mL^{-1}, 50 mg beads mL^{-1}) was added into the BSA blocked EP tube, then 100 μL of first antibody mouse anti-HBsAg (mAb) was added and incubated at 37 °C for 30 min. After that, 200 μL of 1% BSA was added and incubated at 37 °C for 60 min to block nonspecific binding site of MB, the mixture was separated by the magnet and washed with the deionized water three times and then dispersed into 200 μL of PBS (0.01 M, pH 7.4) to obtain the immune complex mAb–mIgG–MB, abbreviated as mAb–MB. After that, magnetic bead immobilized capturing probe was prepared, called as the capturing probe.

2.4. Immune-Detection of HBsAg

100 μL detected antigen HBsAg of different concentrations and 500 μL of the detecting probe dPNP–gAb were firstly mixed and incubated at 37 °C for 30 min. Then 200 μL of the capturing probes mAb–MB was added. After incubation at 37 °C for 30 min, the mixture was separated by magnet, then washed with water and redispersed into 0.5 mL PBS (0.01 M, pH 7.4) to obtain the immune-sandwich complex dPNP–gAb … HBsAg … mAb–MB.

Afterwards, 0.5 mL aforementioned solution and 0.5 mL TPA solution (0.05 mM TPA in PBS buffer of 0.3 mol L^{-1} and pH = 6.8) as co-reactant were added into the ECL detection cell for ECL test. After the immuno-sandwich complex was adsorbed to the surface of the working electrode by a magnet under the electrode, the magnet was moved far away and then its ECL intensity was measured. The corresponding detection conditions were listed as follows: initial potential 0.2 v, sampling rate 10 T s^{-1}, sampling amplification series 3 and photomultiplier voltage 800 V, scanning rate 0.1 v s^{-1}, high potential 1.25 v, low potential 0.2 v, scanning interval 200, scanning sampling interval 0.001, sensitivity 1×10^{-4}. After measuring, washed the detection cell with water three times for next sample detection. The negative control was carried out in the same procedure, but without HBsAg.

3. Results and Discussion

3.1. Morphology, Particle Size Distribution and Spectra

The morphology of the doped polymer nanoparticle dPNP was characterized by TEM (Figure 2A). The results showed that the nanoparticles were well-distributed, no agglomeration was observed during the storage and that the dispersity of the particles was also very good. According to the micro

scale with 200 nm, a particle size of about 20 nm can be estimated. Comparing with the commonly used ECL silica nanoparticles, the prepared nanoparticles had a good dispersity like the silica nanoparticles and also had a much smaller particle size, only about 1/3 of the size of silica nanoparticles [17]. Such a small particle size was much beneficial to reduce the steric hindrance of labeled antibody in immune reaction. A uniform distribution of particle size means that each particle contained almost the same amount of ECL luminophore and then that the particle labeled detection antibodies also had a good uniformity of ECL in the detection.

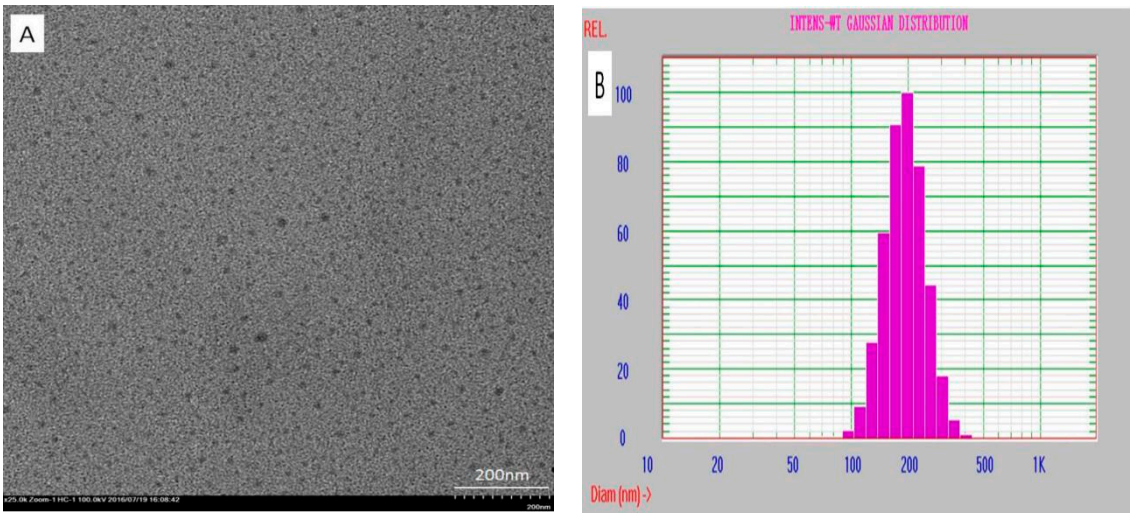

Figure 2. (**A**) TEM image of the dried dPNP and (**B**) the particle size distribution of the hydrated dPNP.

In addition, size distribution of hydrated particle in aqueous medium was also determined by dynamic light scattering (DLS) approach (Figure 2B). The results showed that the particles had a single distribution of average hydrated diameter of 197.5 nm with a narrow range (0.062 in the variance P.I. and 0.55 in chi-squared). It indicated that the particles exhibited a good distribution of particle size in aqueous medium. Compared with the above particle size under the dry state measured by TEM, the size of the hydrated particle increased to about 10 times of the size of its dried particle due to the surface hydration of the particle in the aqueous medium. However, the nanoparticles usually have only about twice increased in size in aqueous medium [17]. This difference should also result from hydration of rich PAA residual chains on the surface of the dPNP, which was similar with the crosslinked PAA on the surface of the nanoparticles [34]. A large number of the carboxyl groups of these PAA residual chains will ionize into carboxyl anions in the aqueous medium, and these anionic chains will stretch far away from the body core of dPNP, because of electrostatic repulsion of these chains. Hence, the particle size of the hydrated dPNP, including the body core and the hydrated layer of residual chain, must increase significantly. Such a hydrated layer of residual chains will be very beneficial to reduce the steric hindrance of immune reaction of the dPNP labeled antibody from the body core of the dPNP.

The characterization of the fluorescence spectra of the dPNP was also investigated. Because the ruthenium derivatives (epo–Ru) grafted on PAA have the characteristic red fluorescence, while there are no fluorescence for the doped polymers PAA and PEI, its fluorescence spectra can be used to characterize the ECL active component epo–Ru on PAA–Ru and in dPNP. The fluorescence spectra of PAA–Ru had shown that the shapes of the excitation and emission spectra and their spectral characteristics were all consistent with epo–Ru, indicating that the grafted PAA maintained the same ECL active component with the small molecule complex epo–Ru and therefore PAA had connected with epo–Ru successfully (Figure S2 in Supporting information). Certainly, the fluorescence spectra of the dPNP were also similar to those of the ruthenium complex epo–Ru (Figure 3), including the

spectral shapes and characteristics, indicating that PAA–Ru was self-assembled into the nanoparticle dPNP successfully.

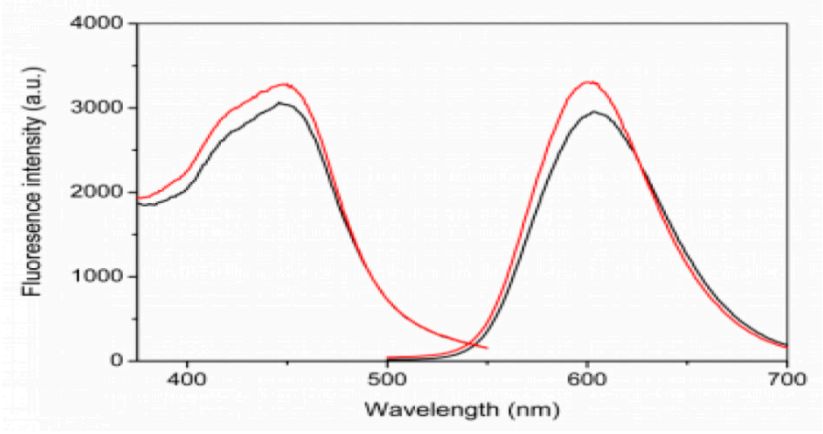

Figure 3. Fluorescent excitation (low wavelength) and emission (high wavelength) spectra of dPNP (red) and ruthenium complex epo–Ru (black).

3.2. ECL Enhancement of the Doped PAA and PEI

Two polymers doped in the nanoparticle dPNP, anionic polyelectrolyte PAA and cationic polymer PEI, played different roles in the ECL enhancement of the nanoparticle. Their ECL intensities were measured according to §2.4. Compared with the undoped polymer nanoparticle PNP, which was self-assembled by the electrostatic and the hydrophobic interaction of PAA–Ru, the added PAA in the PAA–Ru system led to the enhancement of the ECL of PAA-doped nanoparticle paa–PNP (Figure 4). The ECL intensity reached the maximum at the doping amount of 17.4 μg mL^{-1} and decreased as the doping amount was further increased. The results showed that PAA doping could enhance the ECL intensity of the undoped polymer nanoparticle PNP to 109.1%. As PAA is a non-ECL component, so this ECL enhancement should be derived from the polyelectrolyte property of PAA. Due to highly charged anionic long chain of PAA with a high molecular weight of 100 KD, it was able to enhance the electron transfer of the grafted epo–Ru inside the nanoparticles, thus improve the electrical excitation efficiency of the working electrode to the internal grafted epo–Ru. In fact, our previous research on the ion-pair macromolecules PAA–$Ru(bpy)_3^{2+}$ doped SiO_2 nanoparticle has demonstrated that the long chain PAA involved in the non-electroconductive nanoparticle can enhance the electric conductivity of the particle [17]. The decrease of the ECL intensity in higher doping amount of the PAA (more than 17.4 μg mL^{-1}) may be due to the reduction of the relative amount of luminescent polymer PAA–Ru in the doping nanoparticle paa–PNP.

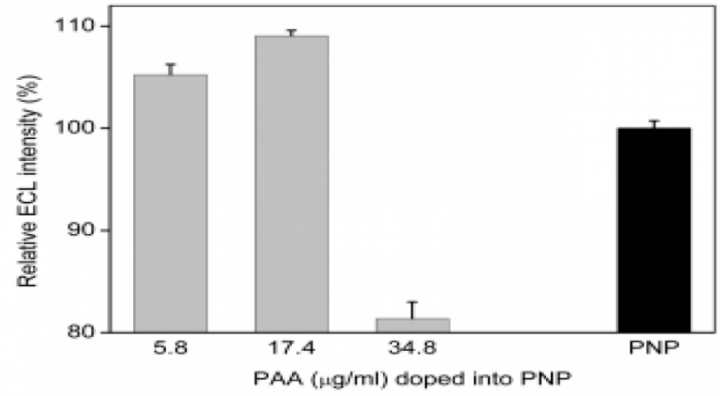

Figure 4. Effect of the doping amount of PAA on the ECL intensity of the polymer nanoparticle PNP.

The effect of the co-doping of the non-luminescent polymer PEI on the ECL of the dPNP was also investigated (Figure 5). It was found that PEI co-doping could further enhance the ECL of PAA-doped polymer nanoparticle paa–PNP, even the PAA doping amount was the above optimized amount of 17.4 μg mL^{-1}. From the results in Figure 5, the ECL intensity of the nanoparticle enhanced with the increase of the amount of doping PEI and when PEI increased to 2.08 μg mL^{-1}, it reached the maximum of the ECL signal to 116.6%, compared with PAA-doped polymer nanoparticle paa–PNP and 127.3% compared with the undoped polymer nanoparticle PNP. Of course, the excessive amount of PEI would also lead to the decrease of the relative content of the ECL component PAA–Ru in the nanoparticles, resulting in the decrease of ECL intensity.

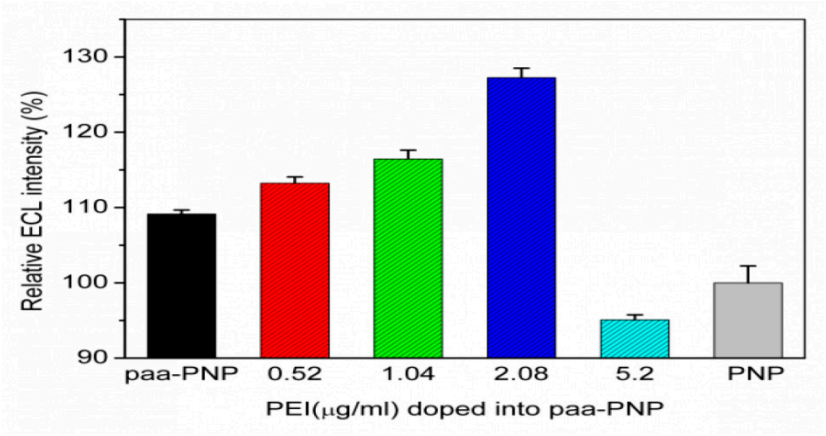

Figure 5. Effect of the doping amount of polymer poly-ethyleneimine (PEI) on the ECL intensity of the PAA-doped polymer nanoparticle paa–PNP.

Obviously, the enhanced efficiency of PEI was better than that of PAA. There should be two reasons for this. On one hand, PEI has a branched structure with rich primary, secondary and tertiary amines and all these numerous tertiary amines in the nanoparticles are analogous to conventional co-reagent TPA which enhanced the ECL intensity significantly. On the other hand, doping PEI enhances the doping efficiency of PAA (see the following Section 3.3) and then this further enhances the electron transfer ability of the ECL active components inside the nanoparticles.

3.3. Effect of Doping Low-Molecular-Weight PEI on Structural Stability of Nanoparticle and Its Good Dispersity

In order to have a good electrical conductivity, PAA must have a long charged chain. Hence, a high molecular weight (MW) of 100 KD was used. Generally speaking, when both anionic and cationic polymers have a long chain and a high-MW, they will quickly accumulate the large volume of cluster to produce sediment in aqueous medium due to electrostatic interaction. To stabilize the structure of the dPNP, PEI embedded in the nanoparticle must have a low-MW. In this study, the cationic polymer PEI of a low-MW of 1.8 KD was used to avoid the sediment successfully. Meanwhile, we noticed that the very short chain of PEI is unable to embed tightly within the long chains of anionic polymers, as electrostatic force of fixing PEI from anionic PAA and PAA–Ru is relatively weak.

Effect of the doping low MW PEI on structural stability of the nanoparticle was investigated by the dynamic light scattering (DLS) approach (Figure 6). When the nanoparticles were stored in the aqueous medium at room temperature and in the dark conditions, the distribution of hydrated-particle size was assayed on the first, seventh and fifteenth days, respectively. The results showed that the particle-size distribution was still stable at 15th day of the storage period and that the corresponding change of the average diameter of the hydrated particle and the two parameters characterizing distribution state, including the variance P.I. (PI) and chi-squared (ChI), were all very small. The corresponding parameters were: 197.5 nm of average diameter, 0.062 in PI and 0.55 in ChI on the first day; 200.9 nm, 0.108 (PI) and 0.62 (ChI) on the 7th day; 213.1 nm, 0.180 (PI) and 0.96 (ChI) on the 15th day. In fact, no

layering and precipitating were observed during the storage period. Most importantly, they all showed single distribution of the diameter of the hydrated particle during the storage and then were able to keep the uniformity of the ECL intensity of the labeled antibody. When the storage time was up to 15 days, no significant swelling of the particles was found, and a little change of the particle size was observed. Hence, the nanoparticle dPNP has a good dispersity in the solution. On the contrary, the undoped and only PAA–Ru self-assembled polymer nanoparticle PNP had a poor distribution on the first day (Figure S3 in Supporting information). The average diameter of the hydrated particle was very large (581.7 nm), which was almost 3 times of the doped nanoparticle dPNP. The parameter ChI characterizing the distribution state was very poor, up to 28.91 and the distribution range of particle diameter was very wide from dozens to 5000 nm. It indicated that the particle structure of PNP was in loose conformation. Clearly, simultaneously doping PAA and PEI enhanced the structural stability of PAA–Ru self-assembled polymer nanoparticle and kept the doped nanoparticle dPNP with an evenly distribution state.

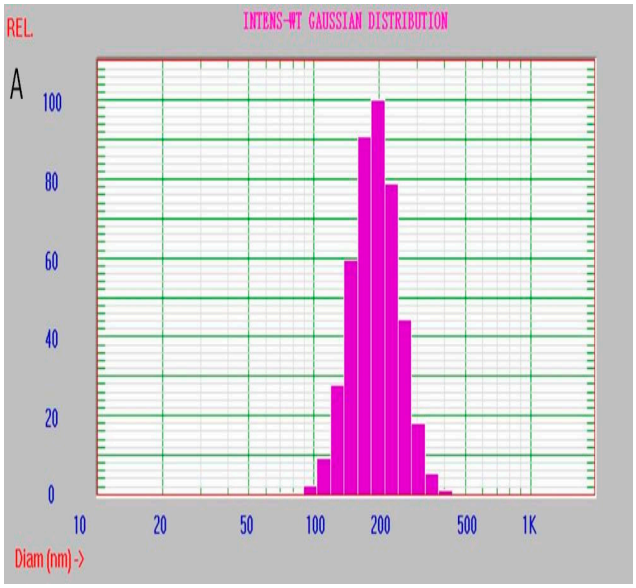

Figure 6. *Cont.*

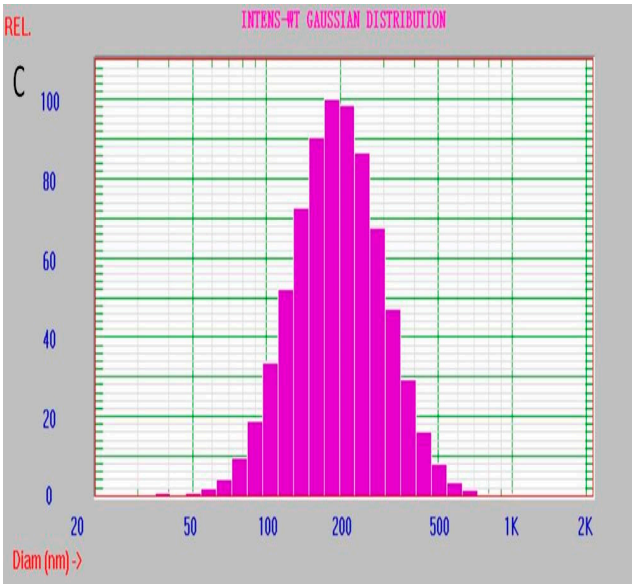

Figure 6. Particle size distribution of the hydrated dPNP at storage day (**A**) 1, (**B**) 7 and (**C**) 15.

The enhancement of the structural stability results from the positive charge characteristics of PEI embedded in the dPNP. As we all know, when there are rich opposite charges on the long chains of two polymers, their electrostatic interaction will be very strong in aqueous medium. PAA–Ru has poor positive charges and poor negative ones on its PAA chain, because a part of the carboxyl groups of the negative charges on the PAA chain was grafted on some molecules of epo–Ru with positive charges. Hence, the electrostatic interaction between any two molecule chains of PAA–Ru in the undoped nanoparticle PNP is weak, and the particle structure of PNP was loose. When PAA and PEI were doped simultaneously, there are not only PEI polymer chains with rich positive charges, but also PAA polymer chains with rich negative charges in the doped nanoparticle dPNP. Compared to the undoped PNP only containing PAA–Ru, the self-assembly procedure would be more effective and the particle structure of the dPNP would be more stable.

3.4. Residual PAA Chains on the Surface of dPNP and Suspension Stability

According to the increase of the hydrated particle size of dPNP about 10 times of its dry size, it was shown that the nanoparticle dPNP has one body core and a large number of the residual chains of PAA on the surface of that body core in the above §3.1. Here the surface charge −11.47 mV (Zeta potential) of the nanoparticle was measured, which also showed that there are the residual chains of PAA on the surface. After dPNP connected antibody by using carboxyl of the residual chain, this residual chain formed a spacer between the labeled antibody and the body core of dPNP and then decreased the steric hindrance of immune reaction of the labeled antibody from the body core [17,27]. In fact, the residual chain of PAA is also beneficial to the suspension stability of dPNP.

The better is the suspension stability of antibody connected nanoparticles in aqueous solution, the more convenient is the storage for a detection reagent, and the better is the reproducibility of detection method. Therefore, we investigated the suspension stability of the dPNP in the solution. The aqueous solution of dPNP was kept in the reagent bottle at room temperature, avoiding light and statically. Meanwhile, drew a line at upper 1/5 of the solution height, which is near the top of the solution, and another line at down 1/5 of the solution height, which is near the bottom of the solution. Moreover, the corresponding solution layers are called as the upper layer and the bottom one, respectively. Under static condition, a small amount of the solutions at the upper and bottom layers of the reagent bottles were sucked out gently on the first, second, third, seventh and thirteenth day, respectively to detect their fluorescence intensities (Figure 7). It was found that the

fluorescence intensities of the upper and the bottom solutions remained almost constant for 13 days, and the intensities did not show a statistical difference between the upper layer and the bottom one. Since the measured fluorescence intensities result from the fluorescent nanoparticles dPNPs in the solution, this indicates that the nanoparticle could uniformly distribute in the solution during long-term storage and had good suspension stability. In fact, this good characteristic should also ascribe to the novel structure of dPNP. The rich residual PAA chains on the surface of dPNP made themselves have rich surface negative charges and good hydrophilicity, thus effectively avoiding the accumulation and precipitation.

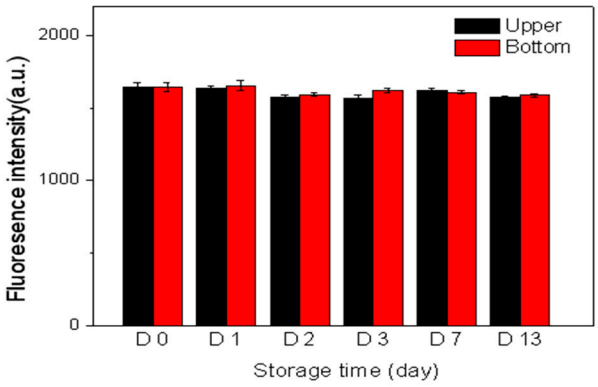

Figure 7. Fluorescent intensities of the upper (**red line)** and bottom (**black line**) solutions of dPNP in the storage bottle at different storage time.

3.5. Optimization of the Labeled Antibody Amount and the Quantitative Analysis of HBsAg

According to the above analysis, we have prepared a nanoparticle well suitable for antibody labeling, immunoassay and the storage, including the small size with uniform distribution, residual PAA chains on the surface, the strong ECL, the good stability of the particle structure, the sufficient suspension stability and the good dispersity. Based on this as-prepared nanoparticle, a sensitive and an accurate immunoassay method were established.

Because of the abundant carboxyl groups on the surface of dPNP, antibodies can be easily labeled by the commonly used EDC-NHS method. Since second antibody IgG was much inexpensive compared with first antibody Ag and could react specifically with the first antibody under a mild condition based on their immunity, the second antibody rabbit anti-goat IgG (gIgG) was first immobilized on the nanoparticle dPNP to obtain dPNP–gIgG. After that, the first antibody goat anti-HBsAg monoclonal antibody (gAb) as the detection antibody was labeled by dPNP–gIgG, to form the immune-complex dPNP–gIgG … gAb based on the immune-reaction between gAb and gIgG. For convenience, it was abbreviated as dPNP–gAb. Optimization of labeled antibody amount (50 μg mL^{-1}) could be found in Section S5 of Supporting information.

In PBS buffer, including the equal amounts of the dPNP-labeled detecting probe dPNP–gAb and the magnetic bead immobilized capturing probe mAb–MB, the concentrations of the detected antigen HBsAg were 1.0, 10.0, 20.0, 50.0 and 100.0 pg $mL^{-1,}$ respectively, and the ECL of the immune complex dPNP–gAb … HBsAg … mAb–MB was detected (Figure 8A). It was found that the ECL intensity of the generated immune complex increased gradually with the increase of the concentration of the detected HBsAg. The standard calibration curve for HBsAg detection is shown in Figure 8B, and the ECL intensity of the generated immune complex was proportional to the concentration of HBsAg in the range from 1.0 to 100.0 pg mL^{-1} (R^2 = 0.9975). The linear regression equation expressed as y = 0.5866x + 57.954, here y is the ECL intensity of the generated immune complex, and x is the concentration of the detected HBsAg. The limit of detection was 0.049 pg mL^{-1} at a signal-to-noise ratio of 3. Compared with the detection limit 0.117 pg mL^{-1} of Reference [17], which is also the same ECL detection system based on magnetic beads, not those sensors based on sensing membrane immobilized on the surface

of working electrode, this approach showed a higher detection sensitivity. It almost achieved the detection sensitivity of the same order of the magnitude as those doped sensing membrane based sensors. This indicated that the ECL detection system of HBsAg based on magnetic bead had also a high sensitivity to ultra-low concentrations of the analyte.

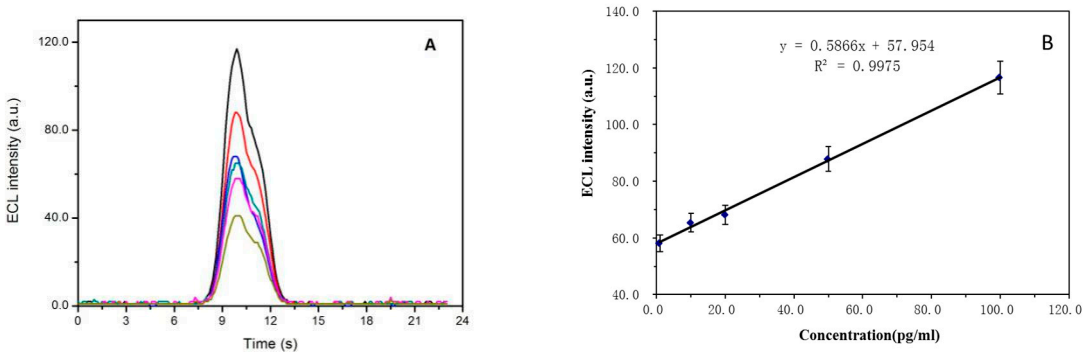

Figure 8. (**A**) ECL intensities of the detected immune complex of the antigen HBsAg at the concentrations of 0.0, 1.0, 10.0, 20.0, 50.0 and 100.0 pg mL^{-1} in the detecting system and (**B**) the corresponding linear relationship between the concentrations of the detected HBsAg and their ECL maximum intensities (n = 3, mean + SD).

3.6. Accuracy and Precision of the Immunoassay

In order to test and verify the accuracy and precision of the proposed ECL immunoassay, sample recovery as a methodological parameter was examined, where two groups of experiments were performed with 25 pg mL^{-1} and 75 pg mL^{-1} of HBsAg. In each group three parallel experiments were carried out, and the mean of three measured ECL intensities and the above linear equation were used to calculate the found concentration (Seen in Table S1 of Supporting information). For the high-concentration group the RSD was 0.167 and for low-concentration group the RSD was 0.058, which indicated that the established analytical system had a high reproducibility and precision. Furthermore, it also showed a high accuracy as the recoveries of two groups were 94.04% and 94.59%, respectively. Actually, for biologic samples, this recovery is quite satisfactory, especially in the ultra-micro detection.

3.7. Assay of Plasma Sample

Usually, HBsAg determination was carried out in a plasma sample, that is, the detected plasma sample must be Hepatitis B positive. However, the assay of Hepatitis B positive plasma samples in general laboratory was strongly forbidden by the laws in China because of the infectivity of the virus. To guarantee the biologic safety, the spiked samples were used to assay HBsAg in plasma, which can also investigate interference for the established method.

In fact, the interferences should be all the components in plasma except for the determined HBsAg, that is HBsAg-negative plasma. Hence, the HBsAg-negative human plasma was used as blank. In this work, a mixed sample of blank plasma was used because the mixed plasma could simulate as many matrix interference components as possible. The blank plasma sample was obtained by mixing the HBsAg-negative plasma samples of ten people, which were provided by Suzhou Blood Center, China. The mixed negative plasma was used to replace PBS buffer in the aforementioned tests. The detected samples of HBsAg-positive plasma were prepared by adding a certain amount of inactivated HBsAg. The low and high concentrations of the two groups were still 25 pg mL^{-1} and 75 pg mL^{-1}, respectively. The corresponding detected concentrations were 22.98 pg mL^{-1} and 68.71 pg mL^{-1} and the corresponding recoveries were 91.90% and 91.61%, and the RSDs were 0.112 (n = 3) and 0.154 (n = 3), respectively. Compared with general requirements (80–120%) for recovery of biologic samples, our recoveries were quite satisfactory, especially in the ultra-micro detection. At the

same time, there also is a good reproducibility. This also proved that plasma components have not obvious interference to assay the contained HBsAg.

4. Conclusions

In this work, an ECL nanoparticle dPNP was prepared by simultaneously doping the long molecular chain of PAA with rich negative charges and the short molecular chain of PEI with rich positive charges based on electrostatic self-assembly. Due to good electrical conductivity of PAA and a large number of tertiary amine groups of PEI, the doped PAA enhanced the ECL intensity of the PNP to 109.1%, and a large number of tertiary amine groups of the doped PEI further enhanced to 127.3%. Due to rich negative charges of PAA and rich positive charges of PEI, the doped PAA and PEI significantly enhanced electrostatic interaction of the self-assembled PAA–Ru with both negative charges and positive ones each other and then significantly increased the structure stability of dPNP. The results showed that the average diameter of the hydrated particle kept almost a constant (197.5–213.1 nm) during long-term storage of 15 days and that the nanoparticles have good suspension stability and good dispersity without detectable aggregation in the solution during the storage. As a result, a highly sensitive ECL immunoassay for HBsAg was developed and the linear range is between 1.0 and 100 pg mL^{-1} with an ultra-low detection limit of 0.049 pg mL^{-1} (S/N = 3). At the same time, the approach had also the good precision, accuracy and selectivity in the analysis of plasma samples.

Supplementary Materials: The following are available online at http://www.mdpi.com/2227-9717/8/9/1054/s1, Figure S1: Synthesizing diagram and structure of $Ru^{2+}(bpy)_2$(phenepoxide), Figure S2: Fluorescent excitation (Upper) and emission (Lower) spectra of epo–Ru (solid line) and PAA–Ru (dashed line), Figure S3: Size distribution of the hydrated polymer nanoparticle PNP, Figure S4. Fluorescence intensity of the supernatant after magnetic separation when adding gIgG at the concentrations of 0 μg mL-1, 20 μg mL-1, 40 μg mL-1, 50 μg mL-1, 70 μg mL-1, respectively, in the immune-reaction system, Table S1: Recovery of HBsAg determined by the built ECL immunoassay (n = 3).

Author Contributions: N.U.A., T.-Y.W., X.-N.W., and T.-H.W. contributed to data curation, material synthesis, characterization, results interpretation, writing and editing. J.-S.Z. and H.-P.X. were as supervision. All authors have read and agreed to the published version of the manuscript.

Funding: This research was supported by the Priority Academic Program Development of the Jiangsu Higher Education Institutes (PAPD).

Conflicts of Interest: The authors declare no conflict of interest.

References

1. Wang, J.; Gao, T.; Wang, F.; Xue, J.; Ye, H.; Xie, M.L. Luteolin improves myocardial cell glucolipid metabolism by inhibiting hypoxia inducible factor-1 alpha expression in angiotensin II/hypoxia-induced hypertrophic H9c2 cells. *Nutr. Res.* **2019**, *65*, 63–70. [CrossRef]
2. Guo, L.C.; Zhu, W.D.; Ma, X.Y.; Ni, H.; Zhong, E.J.; Shao, Y.W.; Yu, J.; Gu, D.M.; Shao, S.D.; Xu, H.D.; et al. Mutations of genes including DNMT3A detected by next-generation sequencing in thyroid cancer. *Cancer Biol. Ther.* **2019**, *20*, 240–246. [CrossRef] [PubMed]
3. Kong, J.H.; Qiu, Y.J.; Li, Y.; Zhang, H.J.; Wang, W.P. TGF-beta 1 elevates P-gp and BCRP in hepatocellular carcinoma through HOTAIR/miR-145 axis. *Biopharm. Drug Dispos.* **2019**, *40*, 70–80. [CrossRef] [PubMed]
4. Cui, X.J.; Sun, X.H.; Lu, F.Q.; Jiang, X.G. Baicalein represses TGF-beta 1-induced fibroblast differentiation through the inhibition of miR-21. *Toxicol. Appl. Pharmacol.* **2018**, *358*, 35–42. [CrossRef] [PubMed]
5. Zeng, Q.; Feng, J.J.; Lu, T.; Xu, L.Y.; Min, C.Y.; Xie, H.P. Influence of Chromatogram Baseline Shifts and Exogenous Metabolite Signals on Metabolic Profiles of Traditional Chinese Medicine Chaihu and Its Liver Toxicity Metabonomics. *Chem. Res. Chin. Univ.* **2017**, *33*, 17–23. [CrossRef]
6. Marquette, C.A.; Blum, L.J. Electro-chemiluminescent biosensing. *Anal. Bioanal. Chem.* **2008**, *390*, 155–168. [CrossRef]
7. Gorman, B.A.; Francis, P.S.; Barnett, N.W. Tris(2,2′-bipyridyl) ruthenium(II) chemiluminescence. *Analyst* **2006**, *13l*, 616–639. [CrossRef]

8. Zhou, X.M.; Zhu, D.B.; Liao, Y.H.; Liu, W.P.; Liu, H.X.; Ma, Z.K.; Xing, D. Synthesis, labeling and bioanalytical applications of a tris(2,2′-bipyridyl) ruthenium(II)-based electrochemiluminescence probe. *Nat. Protoc.* **2014**, *9*, 1146–1159. [CrossRef]
9. Liao, Y.H.; Huang, R.; Ma, Z.K.; Wu, Y.X.; Zhou, X.M.; Xing, D. Target-triggered enzyme-free amplification strategy for sensitive detection of MicroRNA in tumor cells and tissues. *Anal. Chem.* **2014**, *86*, 4596–4604. [CrossRef]
10. Yu, F.L.; Li, G.; Mao, C.M. An electrochemiluminescence aptasensor for tumor cells assay based on signal amplification of Ru(II) covalently doped silica nanoparticles. *Electrochem. Commun.* **2011**, *13*, 1244–1247. [CrossRef]
11. Zanarini, S.; Rampazzo, E.; Ciana, L.D.; Marcaccio, M.; Marzocchi, E.; Montalti, M.; Prodi, F.P.L. Ru(bpy)3 Covalently Doped Silica Nanoparticles as Multicenter Tunable Structures for Electrochemiluminescence Amplification. *J. Am. Chem. Soc.* **2009**, *131*, 2260–2267. [CrossRef] [PubMed]
12. Qian, J.; Zhou, Z.X.; Cao, X.D.; Liu, S.Q. Electrochemiluminescence immunosensor for ultrasensitive detection of biomarker using $Ru(bpy)_3^{2+}$-encapsulated silica nanosphere labels. *Anal. Chim. Acta* **2010**, *665*, 32–38. [CrossRef] [PubMed]
13. Qian, L.; Yang, X.R. One-Step Synthesis of Ru(2,2′-Bipyridine)$_3$Cl$_2$-Immobilized Silica Nanoparticles for Use in Electrogenerated Chemiluminescence Detection. *Adv. Funct. Mater.* **2007**, *17*, 1353–1358. [CrossRef]
14. Yang, X.; Yuan, R.; Chai, Y.Q.; Zhuo, Y.; Mao, L.; Yuan, S.R. $Ru(bpy)_3^{2+}$-doped silica nanoparticles labeling for a sandwich-type electrochemiluminescence immunosensor. *Biosens. Bioelectron.* **2010**, *25*, 1851–1855. [CrossRef]
15. Sardesai, N.P.; Barron, J.C.; Rusling, J.F. Carbon Nanotube Microwell Array for Sensitive Electrochemiluminescent Detection of Cancer Biomarker Protein. *Anal. Chem.* **2011**, *83*, 6698–6703. [CrossRef]
16. Yuan, S.R.; Yuan, R.; Chai, Y.Q.; Mao, L.; Yang, X.; Yuan, Y.L.; Niu, H. Sandwich-type electrochemiluminescence immunosensor based on Ru-silica@Au composite nanoparticles labeled anti-AFP. *Talanta* **2010**, *82*, 1468–1471. [CrossRef]
17. Ge, Z.L.; Song, T.M.; Chen, Z.; Guo, W.R.; Xie, H.P.; Xie, L. Polyelectrolyte-based electrochemiluminescence enhancement for $Ru(bpy)_3^{2+}$ loaded by SiO_2 nanoparticle carrier and its high sensitive immunoassay. *Anal. Chim. Acta* **2015**, *862*, 24–32. [CrossRef]
18. Mao, L.; Yuan, R.; Chai, Y.Q.; Zhuo, Y.; Yang, X. A new electrochemiluminescence immunosensor based on $Ru(bpy)_3^{2+}$-doped TiO_2 nanoparticles labeling for ultrasensitive detection of human chorionic gonadotrophin. *Sens. Actuator B Chem.* **2010**, *149*, 226–232. [CrossRef]
19. Mao, L.; Yuan, R.; Chai, Y.Q.; Zhuo, Y.; Yang, X.; Yuan, S.R. Multi-walled carbon nanotubes and $Ru(bpy)_3^{2+}$ nano-Au nano-sphere as efficient matrixes for a novel solid-state electrochemiluminescence sensor. *Talanta* **2010**, *80*, 1692–1697. [CrossRef]
20. Cao, Y.L.; Yuan, R.; Chai, Y.Q.; Mao, L.; Yang, X.; Yuan, S.R.; Yuan, Y.L.; Liao, Y.H. A solid-state electrochemiluminescence immunosensor based on MWCNTs-Nafion and $Ru(bpy)_3^{2+}$/Nano-Pt nanocomposites for detection of alpha-fetoprotein. *Electroanalysis* **2011**, *23*, 1418–1426. [CrossRef]
21. Yang, X.; Yuan, R.; Chai, Y.Q.; Zhuo, Y.; Mao, L.; Su, H.L.; Yuan, S.R. Electrochemiluminescence sensor based on multi-walled carbon nanotubes doped polyvinyl butyral film containing $Ru(bpy)_3^{2+}$ as chemiluminescence reagent. *Electroanalysis* **2009**, *21*, 1636–1640. [CrossRef]
22. Khramov, A.N.; Collinson, M.M. Electrogenerated chemiluminescence of tris (2,2′-bipyridyl) ruthenium(II) ion-exchanged in nafion-silica composite films. *Anal. Chem.* **2000**, *72*, 2943–2948. [CrossRef] [PubMed]
23. Choi, H.N.; Lee, J.Y.; Lyu, Y.K.; Lee, W.Y. Tris(2,2′-bipyridyl) ruthenium(II) electrogenerated chemiluminescence sensor based on carbon nantube dispersed in sol-gel-derived titania-nafion composite films. *Anal. Chim. Acta* **2006**, *565*, 48–55. [CrossRef]
24. Guo, Z.H.; Dong, S.J. Electrogenerated chemiluminescence from $Ru(Bpy)_3^{2+}$ ion-exchanged in carbon nanotube/perfluorosulfonated ionomer composite films. *Anal. Chem.* **2004**, *76*, 2683–2688. [CrossRef]
25. Zhuang, Y.F.; Ju, H.X. Determination of reduced nicotinamide adenine dinucleotide based on immobilization of tris(2,2′-bipyridyl) ruthenium(II) in multiwall carbon nanotubes/nafion composite membrane. *Anal. Lett.* **2005**, *38*, 2077–2088. [CrossRef]

26. Li, Q.L.; Ding, S.N. Double signal amplification sandwich-structured immunosensor based on TiO_2 nanoparticles enhanced CdSe@ZnS QDs electrochemiluminescence and the dramatic quenching effect of Au@polydopamine nanoparticles. *Sci. Bull.* **2016**, *61*, 931–938. [CrossRef]
27. Dai, P.P.; Li, J.Y.; Yu, T.; Xu, J.J.; Chen, H.Y. Nanocrystal-based electrochemiluminescence sensor for cell detection with Au nanoparticles and isothermal circular double-assisted signal amplification. *Talanta* **2015**, *141*, 97–102. [CrossRef]
28. Cao, J.T.; Wang, H.; Liu, Y.M. Petal-like CdS nanospheres-based electrochemiluminescence aptasensor for detection of IgE with gold nanoparticles amplification. *Spectrocim. Acta Part A Mol. Biomol. Spectrosc.* **2015**, *151*, 274–279. [CrossRef]
29. Xia, H.; Li, L.L.; Yin, Z.Y.; Hou, X.D.; Zhu, J.J. Biobar-Coded Gold Nanoparticles and DNAzyme-Based Dual Signal Amplification Strategy for Ultrasensitive Detection of Protein by Electrochemiluminescence. *ACS Appl. Mater. Interfaces* **2015**, *7*, 696–703. [CrossRef]
30. Liu, Y.M.; Zhou, M.; Liu, Y.Y.; Huang, K.J.; Cao, J.T.; Zhang, J.J.; Shi, G.F.; Chen, Y.H. A novel sandwich electrochemiluminescence aptasensor based on molybdenum disulfide nanosheet-graphene composites and Au nanoparticles for signal amplification. *Anal. Methods* **2014**, *6*, 4152–4157. [CrossRef]
31. Deng, W.P.; Liu, F.; Ge, S.G.; Yu, J.H.; Yan, M.; Song, X.R. A dual amplification strategy for ultrasensitive electrochemiluminescence immunoassay based on a Pt nanoparticles dotted grapheme-carbon nanotubes composite and carbon dots functionalized mesoporous Pt/Fe. *Analyst* **2014**, *139*, 1713–1720. [CrossRef] [PubMed]
32. Wang, X.Y.; Dong, P.; Yun, W.; Xu, Y.; He, P.G.; Fang, Y.Z. A solid-state electrochemiluminescence biosensing switch for detection of thrombin based on ferrocene-labeled molecular beacon aptamer. *Biosens. Bioelectron.* **2009**, *24*, 3288–3292. [CrossRef] [PubMed]
33. Wei, H.; Yin, J.Y.; Wang, E.K. Bis(2,2-bipyridine) (5,6-epoxy-5,6-dihydro-[1,10] phenanthroline) ruthenium: Synthesis and Electrochemical and Electrochemiluminescence Characterization. *Anal. Chem.* **2008**, *80*, 5635–5639. [CrossRef] [PubMed]
34. Cai, X.P.; He, H.H.; Ding, H.Y.; Chen, X.B.; Wei, T.H.; Song, T.M.; You, S.J.; Xie, H.P.; Min, C.Y. Preparation of polyacrylic acid surface-crosslinked strong fluorescent polymer nanoparticles and their sensitive in vitro imaging of cancer cells and long-life in vivo imaging of in situ tumor. *Anal. Methods* **2017**, *9*, 4797–4807. [CrossRef]